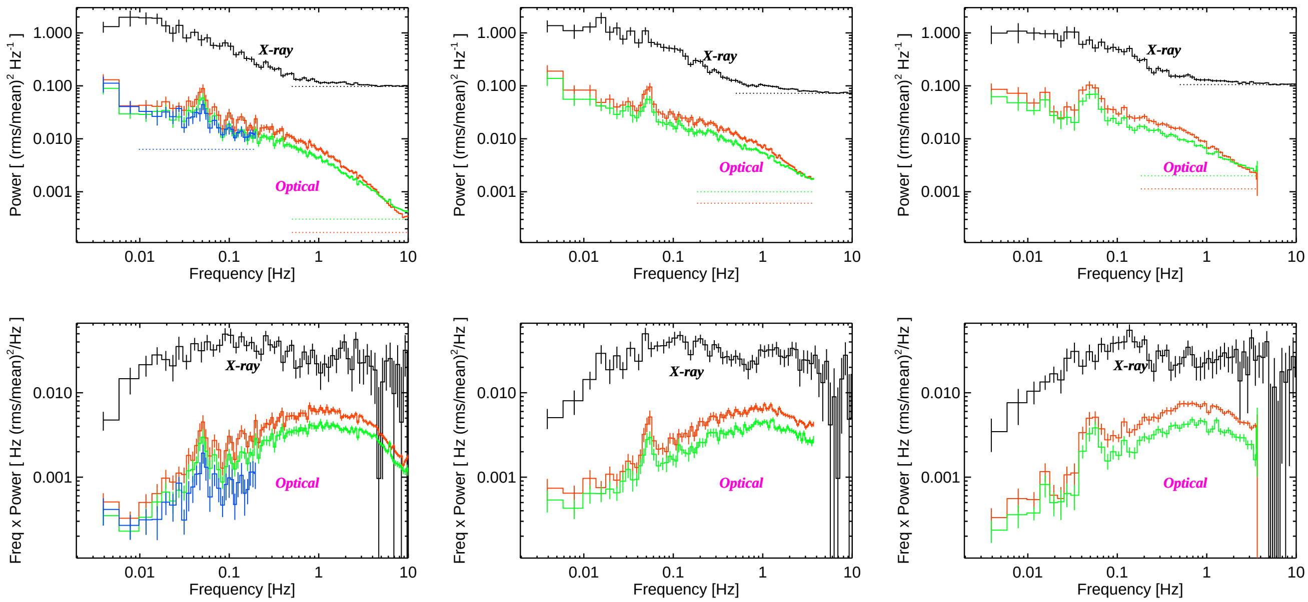

Figure 9. Power spectra of GX 339–4 for Nights 1–3 (from Left to Right). The X-ray full band PSDs are in black, while the optical ones are in red, green and blue for r', g' and u', respectively. The top row shows the PSDs for the net light curves without subtraction of the white noise contribution, which is indicated by the dotted horizontal lines in the respective colours. Power on the y-axis is per unit Hz, with the standard rms-squared normalisation. In these units, the white noise is a constant, and the integral of the PSD over frequency results in the square of the fractional rms amplitude. The bottom row shows the noise-subtracted PSDs, now in units of frequency $\times$ Power.

where t_{j_i}=$t_i+\tau_j$. x and o represent the first and second light curve, in this case the X-ray and optical ones, respectively. The lag τ_j refers to that of the second light curve, with respect to the first, and is itself discretised. Light curves which are related only by a linear transfer function (e.g. a simple time delay or a multiplicative scaling factor) would give a peak CCF value of 1 at the relevant lag time.

The above formula may be used if the two light curves have been extracted on an identical time baseline. This was possible because of the event mode of the *RXTE* PCA, with every single event being recorded. X-ray light curves simultaneous to the optical were obtained by binning the fast (2^{-8} s) barycentred X-ray light curves on the optical baseline, separately for each filter and night. We also checked that direct FTOOLS extraction of X-ray light curves with time bins matching the optical ones, followed by minimal interpolation to the common time baseline, produced unchanged results. Such a methodology is standard procedure in cross-correlation AGN light curves (e.g. Gaskell & Peterson 1987), and has been shown to produce reliable results in the limit of well-sampled data (White & Peterson 1994). As an extra check, we also computed the discrete correlation function (DCF) described by Edelson & Krolik (1988, their Eq. 2). The DCF does not require any interpolation of the data itself, and may be computed using datasets with differing time resolutions. Rather, a correlation is computed between all pairs of data in the two light curves, and a time lag is attached to each pair. The final DCF is then measured by averaging all the pairs that contribute to a binned time lag series. As expected, the match in the CCF shapes between the two methods was excellent for a variety of time lags and X-ray light curve time resolutions. Note that no additional correction for measurement error was applied (cf. White & Peterson 1994); in any case, this would only affect the DCF normalisation.

Each simultaneous light curve was then split into segments 256 s long, which were cross-correlated and then averaged to obtain the final result. The uncertainties on the average at each lag time bin are estimated by error propagation, using the standard deviation of the CCF among these segments. The main CCF structure within absolute lags of several seconds is reproduced on all the nights, with the r' and g' results matching closely in both strength and shape. The most significant other feature is a positive correlation hump around lag=+10 s. Using the coadded signal methodology used for estimating hump significance in the ACFs (§ 4.3), this time between optical lags of +5 and +15 s, results in a signal:noise of 10–30 for this feature between the various nights and the r' and g' filters. Further structures at lags greater than +20 s and below –10 s are also present, though these change dramatically in strength and width between the nights these are not considered to be significant in the full data. The main features have been noted in Paper I with regard to the r' CCF and the overlaid and zoomed-in CCFs from all nights presented in Fig. 1 of that paper make immediately apparent the significance of the main features being discussed (note: in that work, the length of the time segments was not fixed to 256 s, which explains minor differences on long lags with respect to Fig. 15 here, but all the main features appear in both cases). Again, stringent constraints on the evolution of the CCF between the nights must await better datasets, given the changing weather and time resolution of the present observations. In particular, the prominent variation in the CCF on Night 3 on times of several tens of seconds is an artifact of highly variable transparency.

The u' data are much slower; at a time resolution of 2.5 s, each 256 s–long u' band segment has only 103 time bins (as opposed to 5120 bins for the other filters). In Fig. 15, we compare the X-ray vs. u' CCF from Night 1 with slow X-ray vs. r'/g' CCFs, with the latter computed from light curves heavily binned by a factor of 50. Two features stand out from this figure:– i) The u' shows an anti-correlation at small negative lags ($\sim$–5 s) as in the other filters. The